

Improvement of the medical fusion process of images by fuzzy entropy and transformation of the contourlet

Shimaa Janabi, Shaimaa Shukri Abd Alhaleem

Department of Computer Technical Engineering, Faculty of Computer Technical Engineering, Almustafa University College, Baghdad, Iraq

Article Info

Article history:

Received Sep 25, 2021

Revised Mar 8, 2022

Accepted Apr 23, 2022

Keywords:

Fuzzy entropy

Image fusion

Medical image

Nonsampled contourlet transform

Regional energy

ABSTRACT

Many types of medical pictures have to be fused, as single-modality medical images can give limited information because of the imagery and the complicated architecture of the human organ. This study proposes to offer a platform on which to make clinical diagnoses and to increase the accuracy of the target identification and the quality of the fused pictures by combining the benefits of nonsampled contourlet transform (NSCT) and fuzzy entropy. A picture is first broken down into low frequency or high frequency subbands through NSCT. In line with the various features of the low and high frequency components the respective fusion rules must be implemented. It calculates the level of membership of low frequency coefficients. The fusion of coefficients is also calculated and then utilized to retain picture features. By increasing regional energy, high-frequency components are merged. Inverse transformation produces the final fused picture. Experimental results have shown that, based on subjective visual effect and objective assessment standards, the suggested technique produces a satisfactory fusion effect. This process may also achieve high average gradient, standard deviation (SD), and edge preservation and maintain the fused picture features well. Effective reference can be provided by the outcome of the suggested algorithm for patients' assessment.

This is an open access article under the [CC BY-SA](https://creativecommons.org/licenses/by-sa/4.0/) license.



Corresponding Author:

Shimaa Janabi

Department of Computer Technical Engineering, Faculty of Computer Technical Engineering

Almustafa University College

Palestine St., Baghdad, Iraq

Email: shimaa.cte@almustafauniversity.edu.iq

1. INTRODUCTION

For clinical diagnosis, several sorts of medical pictures are supplied. Medical pictures of single modality can only give limited information owing to the imagery and complexity of the architecture of human organ. Various modal pictures therefore need to be merged. This technique takes a picture as a study subject and uses several sources of image information in a fresh image to generate a highly informative profile using particular algorithms [1]. Medical image fusion algorithms address the lack of image information gained through a single imagery mode which allows for full use of supplementary information from each mode and improves the precise diagnosis and the location of lesions of illness [2]. With the advent of fusion technology, multi-scale analytical tools have been presented [3]. Wavelet transform (WT) is the most common technique [4]. However, WT has limitations, including limits, details and texture of pictures, to the capacity to communicate information. In picture fusion, the block effect frequently occurs and decreases fusion quality outcomes. Multi-scale geometric analysis techniques have also been developed for presenting high-order singular features, such as Laplace transformation, curvelet transformation, and

contourlet transformation (CT). Anisotropy and directed selection may effectively be found in the CT theory [5]. This hypothesis has nevertheless numerous weaknesses since image interpolation and removal might lead to the absence of a translation invariance in CT that leads to the occurrence of spectrum aliases [6]. Therefore, Wang *et al.* [7] suggested the CT non-substantiation theory (NSCT). CT is enhanced in this theory to provide an invariance in translation and retains its original benefit. Images are unsure and frequently fuzzy. With its fuzzy logical reasoning, the fuzzy set theory gives a solution and theoretical basis to the fuzziness of images induced by uncertainty [8]. Given that this theory may be used to examine the visual features of pictures, fluctuating technology plays a key part in image processing, given the random nature and human visual properties it addresses [9]. The theory of fuzzy sets is classified by applying the membership of components to evaluate the extent of their affiliation [10], [11]. The uncertainty of picture information is explained by local intuitionist fuzzy entropy, and its magnitude is a crucial foundation to evaluate if a pixel has edges or features. Therefore, it is possible to differentiate the detailed signal and the whole picture characteristic utilizing fuzzy entropy for image fusion. Sugeno was utilized to multimodal medical image fusion using its intuitionist, bizarre set [12]. Fusion of pictures is made possible with intuitionist fuse set technology that improves the brightness and contrast of fused images [13]. Peruru *et al.* [14] provides the fusing procedure for the quality of fusion information, which is based on discrete WT and intuitionist fuzzy sets. With intuitional fuzzy systems to resolve uncertainty the quality of the fused pictures may be dramatically improved. In the field of medical picture fusions, scientists suggested many viable methods [15]. The following two algorithms primarily include: space-based and transformed domains algorithms. Spatial domain-based algorithms do not require complicated picture decomposition and processing but conduct image computation based directly on the original image pixels. These methods are straightforward and can produce useful merge results, although fused pictures can lose information. Image fusion methods are focused mostly on the frequency domain and are more effective than the one-scale fusion approach. This method is based on several areas of transformation.

First, the picture is broken down to yield numerous frequency decomposition coefficients, and various coefficients are subsequently processed on the basis of certain fusion criteria. Common algorithms include transformation of the WT, CT, and discrete cosine. The fusion outcomes are also affected by selection of fusion rules in various transform domains. By evaluating picture characteristics, the selection of appropriate fusion rules is able to improve the fusion outcomes efficiently. Traditional fusion rules include a weighted average process, high absolute value and regional energy. Wan *et al.* were the first to use CS to picture fusion theory [16]. CS theory can enable picture signal dimension to be merged and enhance merging efficiency. Arif and Wang [17] has a fusion technique based on the curvelet transformation that may be used efficiently for goal reconnaissance. Zhu and Bao [18] used the multimodal medical imaging CT-based fusion method. The algorithm can minimize the program's complexity. Gai *et al.* [19] presented a fusion method based on the neural network of impulses and on the transformation of non-sampled shearlet (NSST). The different frequency coefficients were selected according to the inflammatory map. Parvathy *et al.* [20] presented an approach based on NSST image fusion that may capture more picture information than existing multi-scale methods. The multi-scale decomposition method in a medical image fusion algorithm was integrated with the pulse coupled neural network (PCNN) adaptive pulse combined neural network. Although that approach enhances the PCNN algorithm, the final algorithm has limited efficiency [21]. In 1965, Zadeh introduced the idea of fuzzy sets, extensively utilized in a large number of areas. Many academics have investigated the processing of images based on fuzzy sets theory. Imaging technology based on fuzzy may produce better outcomes than standard approaches. This improvement is attributed largely to visual instability, typically owing to fleeting effects. The definitions and description and interpretation of the outcomes of image processing are unclear for edges, regions, textures and other notions. Therefore, it is possible and practicable to use the method of ambiguity in the picture processing. The use of fuzzy theory in the realm of imagery at now focuses mostly on segmentation and development. A new technique based on fugitive logic reasoning is presented; the threshold for the edge identification of digital pictures must not be established in this strategy [22]. This approach also improves the fluidity of the line and curve. Yao reduced the entropy criterion to a minimum to pick an optimum threshold for an image segment [23]. Adaptive approaches for the improvement of images based on NSCT were used and optimisation of artificial bee colonies were employed [24]. A technique for improved images combines histogram equalization with fuzzy set theory, which eliminates the frequent over-improvement and weakening of local information in standard enhancement algorithms [25]. An approach for improving the image, integrating PCNN, and fuzzy theory, has also been developed to boost contrast and visual effects [26]. While fugitive theory is infrequently employed in the field of pictorial fusion, this theory has now gained many academics' interest and has obtained good fusion findings.

On the basis of the aforesaid study, a fusion method is suggested that utilizes fuzzy entropy images to guide NSCT coefficients. The algorithm's particular steps are the following. First, NSCT is utilized to

deconstruct the picture for getting distinct frequency subband coefficients. It calculates the degree of membership and the fluctuation of low frequency coefficients. The fusing of many frequency subband coefficients is then employed by the fuzzy entropy and regional energy. Intensively converted to detect and classified various image data bits and get the fused pictures, the fused coefficients for distinct frequencies. The aforementioned techniques can increase the adequacy of the fusion outcome for medical analysis and observation. The test results verify the superiority of the method presented.

2. METHOD AND MATERIAL

2.1. Fuzzy entropy

There are some distinctions between fuzzy and conventional conceptual conceptions of sets. A degree of membership will be used to indicate the degree to which different types of fuzzy sets belong [27]. First, it will assume a collection of data $X = \{x_1, x_2... X_N\}$, in where (N) is the total classification sample number. (μ_{ik}) is used to represent the degree of (k) sample membership for class I for any data point (x) . The following formula must be met by (μ_{ik}) , expressed as (1) to (3).

$$\forall \mu_{ik} \in [0,1] \tag{1}$$

$$\sum_{i=1}^C \mu_{ik} = 1 \tag{2}$$

$$0 < \sum_{i=1}^C \mu_{ik} = 1 < N \tag{3}$$

The number of clusters where (C) is. By calculating the membership of each pixel with a specified member function, a picture (X) with dimensions of $(R \text{ by } T)$ may be considered as a blurred gateway, expressed as (4).

$$X = \cup_{i=1}^M \cup_{j=1}^N \frac{\mu_{ij}}{x_{ij}}, i = 1,2, \dots, R; j = 1,2, \dots, T \tag{4}$$

The (μ_{ij}/x_{ij}) equation shows the degree to which the (i,j) pixels in an image form a set pixel $\mu_{ij}(0 \leq \mu_{ij} \leq 1)$; and (μ_{ij}) is the ambiguous characteristic of a pixel.

Fuzzy entropy is used to determine a specific area's general ambiguity of the picture. This is the fuzzy entropy measurement of the window $(R \times T)$ as (5), in which (6) and (7).

$$S(i,j) = \frac{1}{R \times T} \sum_i^R \sum_j^T [A(i,j) - B(i,j)] \tag{5}$$

$$A(i,j) = -\mu(x) \log_2 \mu(x) \tag{6}$$

$$B(i,j) = (1 - \mu(x)) \log_2(1 - \mu(x)) \tag{7}$$

Entropy indicates content of information, whereas fuzzy entropy indicates the degree of fluidity [28]. High entropy fluctuation in a specific area shows that the variation in the ambiguity around the pixel is high. Low-fuzzy entropy refers to small changes in the region and is a flat area. Figure 1 shows the Fuzzy-entropy histogram of a magnetic resonance tomography (MRT) image, where Figure 1(a) is the utilized MRT image and Figure 1(b) is the fuzzy-entropy histogram of the image.

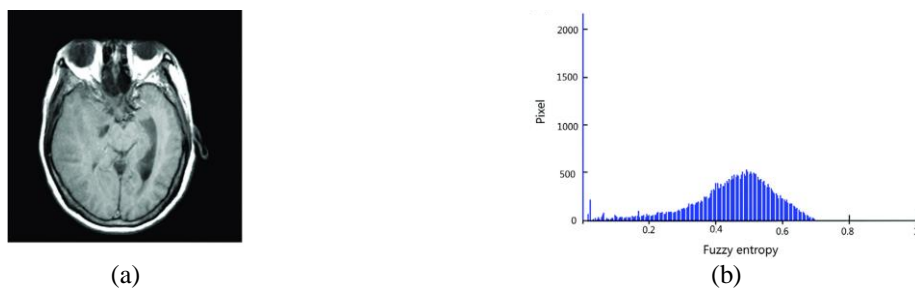


Figure 1. The fuzzy-entropy histogram of an MRT image for (a) the utilized MRT image and (b) the fuzzy-entropy histogram of the image

2.2. Non-subsampling contourlet transform

CT-based NSCT is proposed and implemented by means of non-desampled decomposition of the laplace pyramid (LP) and directional filter banks not sampled [29]. Figure 2 displays NSCT's structure. Image breakdown depending on the following two components are included in NSCT: multiscale and decompositions multidirectional. First of all, a non-sampled pyramid decomposes the original picture nonsubsampling pyramid filter bank (NSPFB) for low and high-pass band obtaining filter bank images. The nonsubsampling directional filter bank (NSDFB) is then utilized to deconstruct the source picture. The source image is then decomposed. The high-pass subband picture is broken down into multi-layer subband images to deconstruct the multi-directional image. Finally, the decomposition of the multilayer subband results by repeating the aforementioned procedures for each picture with a low pass. NSDFB and NSPFB degradations in NSCT lack LP degradation in CT and filter downsampling in the direction filter bank degradation and extensive filtering.

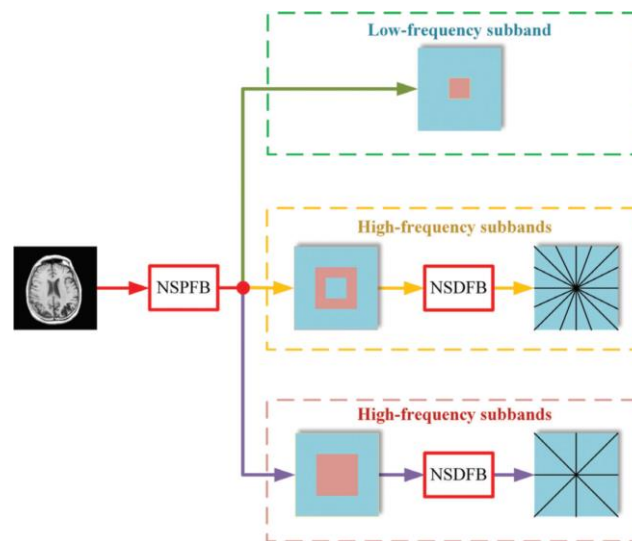


Figure 2. Structure of NSCT

All NSCT subbands of decomposition are merged using filter banks downsampling. The picture in the subband has the same size and invariance of translation. The subband picture therefore exhibits high multiscale and multi-direction, thereby avoiding the Gibbs. NSCT transforms the two source pictures (I^i) and (I^v) with the following terms as (8) and (9).

$$I^i = L^i(x, y) + \sum_{j=1}^J H_{j,r}^i(x, y) \quad (8)$$

$$I^v = L^v(x, y) + \sum_{j=1}^J H_{j,r}^v(x, y) \quad (9)$$

After decomposition it is possible to extract the (H) high-frequency and (L) low-frequency coefficients. In the formula, (J) refers to the number of layers of decomposition, (j) refers to the scale size and (r) refers to the direction.

2.3. Strategy for high-frequency subbands

After NSCT decomposition, the approximation information left in the HF coefficients is diminished. The high-frequency fusion coefficients are useful data. The region energy can take into account the correlation between the pixels in the region and can further reflect the local features of the picture. The centre pixel with wide range energy shows the evident characteristics of the image. This article thus chose guidelines for fusing pictures based on regional energy. First of all, the centre pixels (x, y), the specified size (R by T) is the regional block and the region's energy is calculated, expressed as (10).

$$E(x, y) = \frac{1}{R \times T} \sum_{m=1}^R \sum_{n=1}^T H_{j,r}^2(x_m, y_n) \quad (10)$$

The merging of high frequency signals is then performed Maximizing energy for the region. The regulations are like (11).

$$H_{j,r}^r(x,y) = \begin{cases} H_{j,r}^i(x,y), E_{j,r}^i(x,y) > E_{j,r}^v(x,y) \\ H_{j,r}^v(x,y), else \end{cases} \tag{11}$$

2.4. Strategy for low-frequency subbands

Most picture energy is represented by low-frequency coefficients. This study mixes these coefficients with regional entropy size calculation. First of all, Gauss's function calculates the membership degree of the low frequency coefficient. The Gaussian function is intuitive, the computation is straightforward, the curve is smooth and hence extensively utilized. The following is the expression as (12).

$$\mu(x,y) = e^{-|L(x,y)-c|^2/2\sigma^2} \tag{12}$$

In which $L(x,y)$ is the gray value of a point and the regional mean and variance centered on (L) is marked with (c) and (σ^2) correspondingly. Finally, the fuzzy entropy $S(i,j)$ in the region (i) determined using (5). The region chosen for this investigation is three by three in size. A significant entropy in the region shows a major change in texture and the presence of edge information in the region.

In contrast, a modest local entropy in the area shows that the picture may belong to the flat area and has general characteristics. Appropriate entropy thresholds are determined by this study with the mean value S and SD std of a fused picture. The following rules are expressed as (13) and (14), The fusion rule is as (15), where expressed as (16) and (17). The suggested NSCT based and fuzzy entropy fusion technique is shown in Figure 3.

$$thr1 = S \tag{13}$$

$$thr2 = S + std \tag{14}$$

$$L^r = \begin{cases} L^i(x,y), S^i > thr2S^v < thr1 \\ L^v(x,y), S^v > thr2S^i < thr1 \\ \sigma^i L^i(x,y) + \sigma^v L^v(x,y), else \end{cases} \tag{15}$$

$$\sigma^i = \frac{S^i(x,y)}{S^i(x,y) + S^v(x,y)} \tag{16}$$

$$\sigma^v = 1 - \sigma^i \tag{17}$$

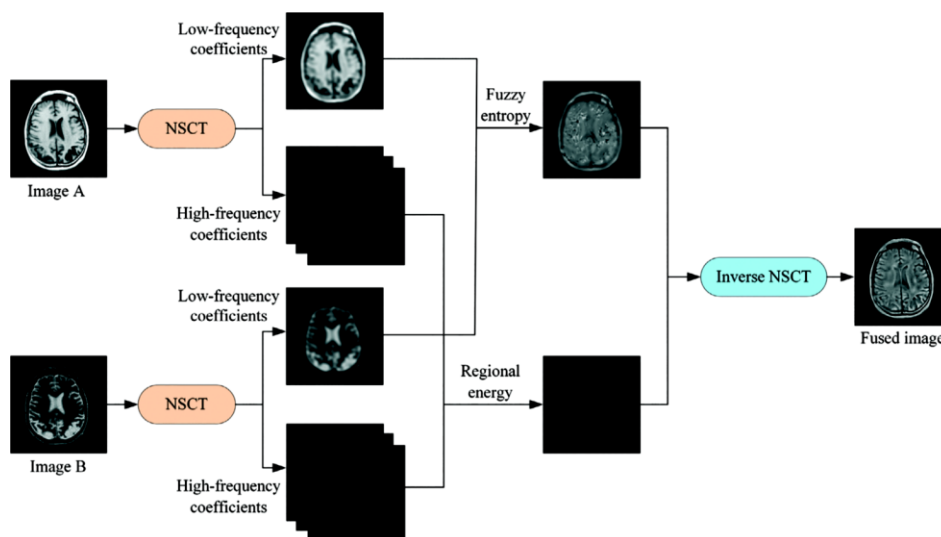


Figure 3. Flowchart of the medical image fusion method

3. RESULTS

The algorithm proposed is simulated in order to show its correctness on the MATLAB platform. The benefit of the fusion method is checked by fusion and comparison in references [4], [5], [30]–[33] of medical images with image fusion algorithms. An image fusion algorithm based on wavelet transform is used in [4]. A fusion algorithm based on contourlet transform and weighted regional variance is applied in [5]. Arif and Wang [17] uses an image fusion technique based on transforming the curvelet and Laplacian energy. Wang *et al.* [30] uses a fusion technique based on consistency between WT and the neighbourhood. Ellmauthaler *et al.* [32] uses an NSCT fusion algorithm and regional energy. Cai *et al.* [33] uses an NSST-based picture fusion method with neighbourhood structure characteristics. NSCT is divided into three levels, with eight orientations in each. In this investigation. For pyramid and scale breakdown filters "9/7" and "pkva" are respectively accepted. The fusion results from various algorithms are shown in Figures 4–6. The picture of the CT shows skeletal information and lesions. The image is computed tomographic. Their impact on the soft tissue of the injury itself is, however, weak, whereas the soft tissue and its lesions are shown effectively in the picture of the MRT. The tissue may be acquired in detail at several angles and plane.

This figure helps to grasp the focal details; however, the image of the skeleton is fluffy. The merging of images of CT and MRT can be used to diagnose and locate disease. In Figures 4(a)–(i) the fusion results on pictures of a male patient with speech problem and an acute stroke are shown. Figures 4(a) and (b) are the original MRT and CT images of the patient. Fusion results pictures in Figure 5 from a male with left occipital infarction are shown in Figures 5(a)–(i). Figures 5(a) and (b) are the original MRT and CT images of the patient. Fusion results pictures of a woman with Alzheimer's illness and serious focal contractions in the lateral area are presented in Figure 6. Figures 6(a) and (b) are the original MRT and CT images of the patient correspondingly. The fusion picture is assessed objectively by using the mean gradient (AG), spatial frequency (SF), edge protection ($Q^{AB/F}$), and SD. Clarity is also known as AG. Large AG values show excellent clarity of picture [34]. SF shows the merged image's sharpness. A big SF shows excellent clarity of the picture. The quantity of high frequency fusion information may be calculated using the ($Q^{AB/F}$) picture [20]. The large values of ($Q^{AB/F}$) show good outcomes of fusion. The picture contrast is changed by SD [35]. Large SD values show the distinct outlines of the edge [36]–[38].

Two pictures were successfully merged by the seven algorithms in Figures 4 to 6. Fused pictures are capable of observing skeletal tissue information, soft tissue information, and lesions and further analysis based on the outcome. By comparison, the general image quality of Figures 4(c), 5(c), and 6(c) is flat and poor in contrast. Figures 4(d), 5(d), and 6(d) have improved outcomes compared to Figures 4(c), 5(c), and 6(c).

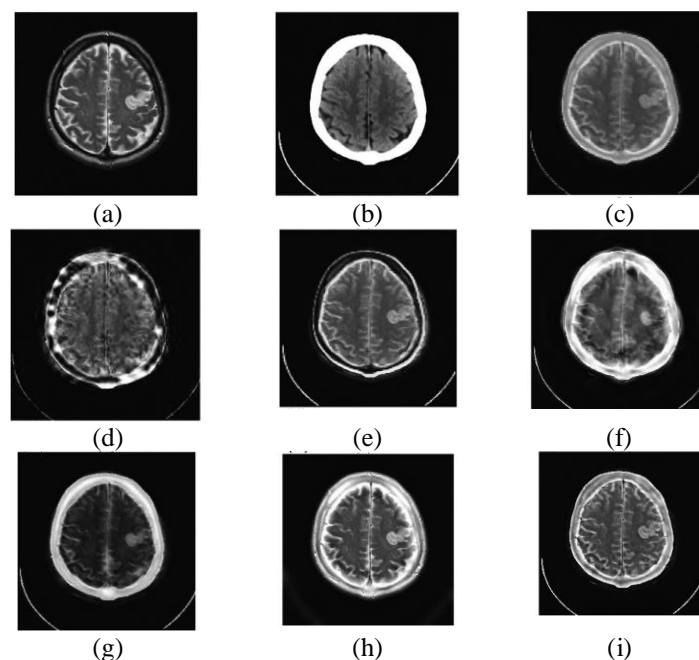


Figure 4. Fusion results of: (a) MRT2 image, (b) CT image, (c) result of reference [4], (d) result of reference [5], (e) result of reference [30], (f) result of reference [17], (g) result of reference [32], (h) result of reference [33], and (i) result of the proposed method

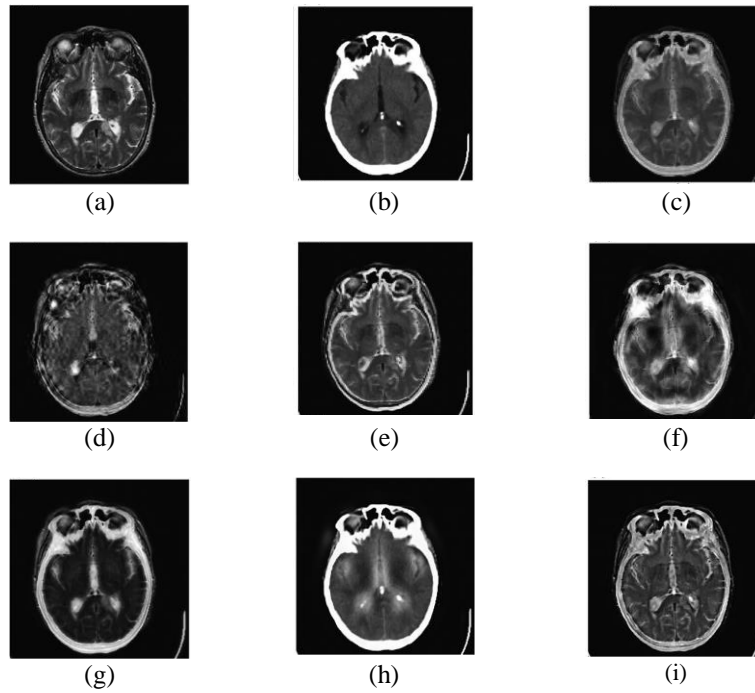


Figure 5. Fusion results of: (a) MRT2 image, (b) CT image, (c) result of reference [4], (d) result of reference [5], (e) result of reference [30], (f) result of reference [17], (g) result of reference [32], (h) result of reference [33], and (i) result of the proposed method

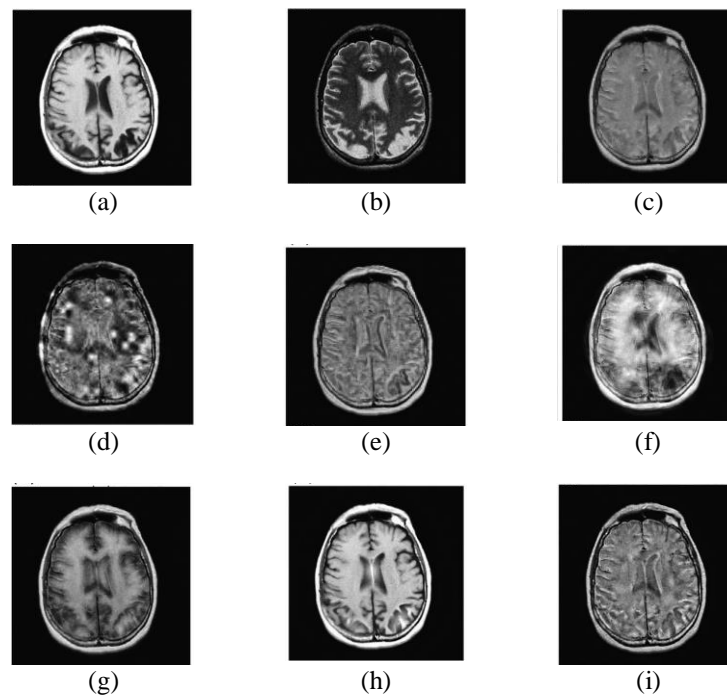


Figure 6. Fusion results of: (a) MRT2 image, (b) CT image, (c) result of reference [4], (d) result of reference [5], (e) result of reference [30], (f) result of reference [17], (g) result of reference [32], (h) result of reference [33], and (i) result of the proposed method

While the contrast of the image is considerably enhanced, details of the texture are unclear. Dark pictures with poor contrast are seen in Figures 4(e), 5(e), and 6(e). These features do not promote visual observation. The picture spatial information can successfully be preserved in Figures 4(f), 5(f), and 6(f), although CT brain features are not apparent. Figures 4(g), 5(g), and 6(g) blur the soft tissue border. Image

details cannot be successfully preserved in Figures 4(h), 5(h), and 6(h). The edge and texture of the suggested algorithm, by comparison, are rich. In addition, this method provides a greater level of contrast and clarity than other algorithms are acquired. This enables clinicians to assess patient condition effectively with the findings of the suggested algorithm.

The SF and ($Q^{AB/F}$) values of the picture are low and indicate their inadequate detail based on the algorithm referred to in references [4], [32]. The fusion picture based on the references [5], [30] algorithms reveal significant changes in the indications in question. The low SD of this image of fusion nevertheless shows the poor contrast. The image's SD is high and means an abundance of information based on the method provided by references [31], [33]. Other indications, however, were behind those of the image fused using the method provided. The objective assessment results further demonstrate that rich information, clarity, contrast and extra picture characteristics are contained in the fusion results of the given technique.

4. CONCLUSION

In line with the features of multimodal medical pictures, a NSCT-based fusion method is given. This technique utilizes fluid entropy to control picture fusion in the subband of low frequency and maximal local energy for fusion in high-frequency areas. The NSCT is very directive and has smooth edges properly conveyed. Furthermore, in the extraction of picture contours and forms, the performance of the suggested method is greater than that of previous techniques. The image fuzzy entropy can efficiently represent unclear image data and properly differentiate signal details and overall picture characteristics. The resulting technique improves the AG, SF, and ($Q^{AB/F}$) by 14,4%–19,7%–18,9%–30,9%– and 13,3% by 51,2% correspondingly respectively. This way picture data may be efficiently retained and high-quality photos are produced. The algorithm's high flexibility is demonstrated through subjective and objective analyses. The algorithm can also give reliable medical diagnostic judgment information. In the future it will be helpful to reduce the time required, increase the algorithm efficiency further and pick adequate fusion rules.





REFERENCES

- [1] Y. Liu, L. Wang, J. Cheng, C. Li, and X. Chen, "Multi-focus image fusion: a survey of the state of the art," *Information Fusion*, vol. 64, pp. 71–91, Dec. 2020, doi: 10.1016/j.inffus.2020.06.013.
- [2] L. Armi and S. Fekri-Ershad, "Texture image classification based on improved local quinary patterns," *Multimedia Tools and Applications*, vol. 78, no. 14, pp. 18995–19018, Jul. 2019, doi: 10.1007/s11042-019-7207-2.
- [3] J. Zhao *et al.*, "Automatic segmentation and reconstruction of coronary arteries based on sphere model and Hessian matrix using CCTA images," *Journal of Physics: Conference Series*, vol. 1213, no. 4, p. 042049, Jun. 2019, doi: 10.1088/1742-6596/1213/4/042049.
- [4] O. Prakash, C. M. Park, A. Khare, M. Jeon, and J. Gwak, "Multiscale fusion of multimodal medical images using lifting scheme based biorthogonal wavelet transform," *Optik*, vol. 182, pp. 995–1014, Apr. 2019, doi: 10.1016/j.ijleo.2018.12.028.
- [5] L. Jiao, "An image denosing algorithm for strong noise image based on structural similarity of contourlet domain via grey relational analysis," in *Innovative Mobile and Internet Services in Ubiquitous Computing*, Eds. Cham: Springer, 2020, pp. 300–309.
- [6] X. Zhuang *et al.*, "Evaluation of algorithms for multi-modality whole heart segmentation: an open-access grand challenge," *Medical Image Analysis*, vol. 58, p. 101537, Dec. 2019, doi: 10.1016/j.media.2019.101537.
- [7] Z. Wang, X. Li, H. Duan, Y. Su, X. Zhang, and X. Guan, "Medical image fusion based on convolutional neural networks and non-subsampled contourlet transform," *Expert Systems with Applications*, vol. 171, p. 114574, Jun. 2021, doi: 10.1016/j.eswa.2021.114574.
- [8] A. P. Wei, D. F. Li, B. Q. Jiang, and P. P. Lin, "The novel generalized exponential entropy for intuitionistic fuzzy sets and interval valued intuitionistic fuzzy sets," *International Journal of Fuzzy Systems*, vol. 21, no. 8, 2019, doi: 10.1007/s40815-019-00743-6.
- [9] P. Mittal, R. K. Saini, and N. K. Jain, "Image enhancement using fuzzy logic techniques," in *Soft Computing: Theories and Applications*, K. Ray, T. K. Sharma, S. Rawat, R. K. Saini, and A. Bandyopadhyay, Eds. Singapore: Springer, 2019, pp. 537–546, doi: 10.1007/978-981-13-0589-4_50.
- [10] M. Abd Elaziz, U. Sarkar, S. Nag, S. Hinojosa, and D. Oliva, "Improving image thresholding by the type II fuzzy entropy and a hybrid optimization algorithm," *Soft Computing*, vol. 24, no. 19, pp. 14885–14905, Oct. 2020, doi: 10.1007/s00500-020-04842-7.
- [11] H. Chen, H. Qiao, L. Xu, Q. Feng, and K. Cai, "A fuzzy optimization strategy for the implementation of RBF LSSVR model in Vis-NIR analysis of pomelo maturity," *IEEE Transactions on Industrial Informatics*, vol. 15, no. 11, 2019, doi: 10.1109/TII.2019.2933582.
- [12] B. O. Adame, A. O. Salau, B. C. Subbanna, T. Tirupal, and S. F. Sultana, "Multimodal medical image fusion based on intuitionistic fuzzy sets," in *Proceedings of 2020 IEEE International Women in Engineering (WIE) Conference on Electrical and Computer Engineering, WIECON-ECE 2020*, Dec. 2020, pp. 131–134, doi: 10.1109/WIECON-ECE52138.2020.9397963.
- [13] T. Tirupal, B. G. K. Mohan, and S. S. Kumar, "Multimodal medical image fusion based on yager's intuitionistic fuzzy sets," *Iranian Journal of Fuzzy Systems*, vol. 16, no. 1, pp. 33–48, 2019.
- [14] P. Peruru and D. Madhavi, "Multimodal medical image fusion based on undecimated wavelet transform and fuzzy sets," *International Journal of Innovative Technology and Exploring Engineering*, vol. 8, no. (6), 2019.
- [15] H. Ullah, B. Ullah, L. Wu, F. Y. O. Abdalla, G. Ren, and Y. Zhao, "Multi-modality medical images fusion based on local-features fuzzy sets and novel sum-modified-Laplacian in non-subsampled shearlet transform domain," *Biomedical Signal Processing and Control*, vol. 57, p. 101724, Mar. 2020, doi: 10.1016/j.bspc.2019.101724.
- [16] M. Ghahremani, Y. Liu, P. Yuen, and A. Behera, "Remote sensing image fusion via compressive sensing," *ISPRS Journal of Photogrammetry and Remote Sensing*, vol. 152, pp. 34–48, Jun. 2019, doi: 10.1016/j.isprsjprs.2019.04.001.
- [17] M. Arif and G. Wang, "Fast curvelet transform through genetic algorithm for multimodal medical image fusion," *Soft Computing*, vol. 24, no. 3, pp. 1815–1836, Feb. 2020, doi: 10.1007/s00500-019-04011-5.





- [18] X. Zhu and W. Bao, "Investigation of remote sensing image fusion strategy applying PCA to wavelet packet analysis based on IHS transform," *Journal of the Indian Society of Remote Sensing*, vol. 47, no. 3, pp. 413–425, Mar. 2019, doi: 10.1007/s12524-018-0930-8.
- [19] D. Gai, X. Shen, H. Cheng, and H. Chen, "Medical image fusion via PCNN based on edge preservation and improved sparse representation in NSST domain," *IEEE Access*, vol. 7, pp. 85413–85429, 2019, doi: 10.1109/ACCESS.2019.2925424.
- [20] V. S. Parvathy, S. Pothiraj, and J. Sampson, "A novel approach in multimodality medical image fusion using optimal shearlet and deep learning," *International Journal of Imaging Systems and Technology*, vol. 30, no. 4, pp. 847–859, Dec. 2020, doi: 10.1002/ima.22436.
- [21] X. Li and J. Zhao, "A novel multi-modal medical image fusion algorithm," *Journal of Ambient Intelligence and Humanized Computing*, vol. 12, no. 2, pp. 1995–2002, Feb. 2021, doi: 10.1007/s12652-020-02293-4.
- [22] N. Ahmadi, "Intelligent approaches towards fuzzy segmentation and fuzzy edge detection," *Journal of Soft Computing and Decision Support Systems*, vol. 6, no. 6, pp. 9–13, 2019.
- [23] S. Dhar and M. K. Kundu, "Interval type-2 fuzzy set and human vision based multi-scale geometric analysis for text-graphics segmentation," *Multimedia Tools and Applications*, vol. 78, no. 16, pp. 22939–22957, Aug. 2019, doi: 10.1007/s11042-019-7649-6.
- [24] A. Asokan and J. Anitha, "Artificial bee colony-optimized contrast enhancement for satellite image fusion," in *Artificial Intelligence Techniques for Satellite Image Analysis*, D. J. Hemanth, Ed. Cham: Springer, pp. 83–105, 2020.
- [25] A. Paul, T. Sutradhar, P. Bhattacharya, and S. P. Maity, "Infrared images enhancement using fuzzy dissimilarity histogram equalization," *Optik*, vol. 247, p. 167887, Dec. 2021, doi: 10.1016/j.ijleo.2021.167887.
- [26] Z. Qu, Y. Xing, and Y. Song, "Image enhancement based on pulse coupled neural network in the nonsubsample shearlet transform domain," *Mathematical Problems in Engineering*, vol. 2019, pp. 1–11, Feb. 2019, doi: 10.1155/2019/2641516.
- [27] X. Chu, Z. Zhou, C. Yang, and X. Xiang, "Adaptive smoothness constraint image multilevel fuzzy enhancement algorithm," *Sains Malaysiana*, vol. 48, no. 12, pp. 2777–2785, Dec. 2019, doi: 10.17576/jsm-2019-4812-19.
- [28] F. Zhao, H. Hu, Y. Chen, J. Liang, X. He, and Y. Hou, "Accurate segmentation of heart volume in CTA with landmark-based registration and fully convolutional network," *IEEE Access*, vol. 7, pp. 57881–57893, 2019, doi: 10.1109/ACCESS.2019.2912467.
- [29] K. B. Lee and H. W. Goo, "Comparison of quantitative image quality of cardiac computed tomography between raw-data-based and model-based iterative reconstruction algorithms with an emphasis on image sharpness," *Pediatric Radiology*, vol. 50, no. 11, pp. 1570–1578, Oct. 2020, doi: 10.1007/s00247-020-04741-x.
- [30] Z. Wang, X. Li, H. Duan, X. Zhang, and H. Wang, "Multifocus image fusion using convolutional neural networks in the discrete wavelet transform domain," *Multimedia Tools and Applications*, vol. 78, no. 24, pp. 34483–34512, 2019, doi: 10.1007/s11042-019-08070-6.
- [31] R. Wang, N. Fang, Y. He, Y. Li, W. Cao, and H. Wang, "Multi-modal medical image fusion based on geometric algebra discrete cosine transform," *Advances in Applied Clifford Algebras*, vol. 32, no. 2, p. 19, Apr. 2022, doi: 10.1007/s00006-021-01197-6.
- [32] A. Ellmauthaler, C. L. Pagliari, E. A. B. da Silva, J. N. Gois, and S. R. Neves, "A visible-light and infrared video database for performance evaluation of video/image fusion methods," *Multidimensional Systems and Signal Processing*, vol. 30, no. 1, pp. 119–143, Jan. 2019, doi: 10.1007/s11045-017-0548-y.
- [33] H. Cai, L. Zhuo, X. Chen, and W. Zhang, "Infrared and visible image fusion based on BEMSD and improved fuzzy set," *Infrared Physics and Technology*, vol. 98, pp. 201–211, May 2019, doi: 10.1016/j.infrared.2019.03.013.
- [34] P. Mangalraj, V. Sivakumar, S. Karthick, V. Haribaabu, S. Ramraj, and D. J. Samuel, "A review of multi-resolution analysis (MRA) and multi-geometric analysis (MGA) tools used in the fusion of remote sensing images," *Circuits, Systems, and Signal Processing*, vol. 39, no. 6, pp. 3145–3172, Jun. 2020, doi: 10.1007/s00034-019-01316-6.
- [35] V. Radhika and V. K. Guru, "Image fusion method based on regional feature and improved bi-dimensional intrinsic mode function," *i-manager's Journal on Image Processing*, vol. 7, no. 3, p. 14, 2020, doi: 10.26634/jip.7.3.17674.
- [36] Z. Liu, E. Blasch, and V. John, "Statistical comparison of image fusion algorithms: recommendations," *Information Fusion*, vol. 36, pp. 251–260, Jul. 2017, doi: 10.1016/j.inffus.2016.12.007.
- [37] N. Ismail, I. Nursalim, H. M. Saputra, and T. S. Gunawan, "Implementation of fuzzy logic control system on rotary car parking system prototype," *Indonesian Journal of Electrical Engineering and Computer Science*, vol. 12, no. 2, pp. 706–715, Nov. 2018, doi: 10.11591/ijeecs.v12.i2.pp706-715.
- [38] G. Joshi and A. J. P. Pius, "ANFIS controller for vector control of three phase induction motor," *Indonesian Journal of Electrical Engineering and Computer Science*, vol. 19, no. 3, pp. 1177–1185, Sep. 2020, doi: 10.11591/ijeecs.v19.i3.pp1177-1185.

BIOGRAPHIES OF AUTHORS



Shimaa Janabi     received B.Eng. and M.Sc degrees in electronics and communication engineering from Al-Nahrain University, Iraq, in 2013 and 2020, respectively. Currently, she is an Associate Lecturer at the Department of Computer Technical Engineering, Almustafa University College. Her research interests include image processing, computer programming, fuzzy algorithm, power electronics, medical image enhancement, and application of image processing techniques in medical imaging. She can be contacted at email: Shimaa.cte@almustafauniversity.edu.iq.



Shaimaa Shukri Abd Alhaleem     holds a B.Sc in electrical engineering and a M.Sc in power engineering from university of technology, Baghdad, Iraq. She is currently department rapporteur of the computer technical engineering department at Almustafa university college. Her research interests include renewable energy, power quality, high quality utility interface, power electronics, power generation, power grids, power supply quality, power transmission reliability, relay protection, power system stability, power transmission lines, power transmission planning, power transmission protection, battery chargers, and circuit breakers. She can be contacted at email: shaimaa.cet@almustafauniversity.edu.iq.